Molecular Dynamics Simulations of a Protein on Hydrophobic and Hydrophilic Surfaces

Douglas J. Tobias,*# Wen Mar,* J. Kent Blasie,* and Michael L. Klein*
*Department of Chemistry, University of Pennsylvania, Philadelphia, Pennsylvania 19104-6323, and #Reactor Radiation Division, Materials Science and Engineering Laboratory, National Institute of Standards and Technology, Gaithersburg, Maryland 20899-0001 USA

ABSTRACT Molecular dynamics simulations have been used to investigate the behavior of the peripheral membrane protein, cytochrome *c*, covalently tethered to hydrophobic (methyl-terminated) and hydrophilic (thiol-terminated) self-assembled monolayers (SAMs). The simulations predict that the protein will undergo minor structural changes when it is tethered to either surface, and the structures differ qualitatively on the two surfaces: the protein is less spherical on the hydrophilic SAM where the polar surface residues reach out to interact with the SAM surface. The protein is completely excluded from the hydrophobic SAM but partially dissolves in the hydrophilic SAM. Consequently, the surface of the thiol-terminated SAM is considerably less ordered than that of the methyl-terminated SAM, although a comparable, high degree of order is maintained in the bulk of both SAMs: the chains exhibit collective tilts in the nearest-neighbor direction at angles of 20° and 17° with respect to the surface normal in the hydrophobic and the hydrophilic SAMs, respectively. On the hydrophobic SAM the protein is oriented so that the heme plane is more nearly parallel to the surface, whereas on the hydrophilic surface it is more nearly perpendicular. The secondary structure of the protein, dominated by α helices, is not significantly affected, but the structure of the loops as well as the helix packing is slightly modified by the surfaces.

INTRODUCTION

Structural studies of reconstituted membrane–protein systems provide data for the discussion of supramolecular organization and function in complex assemblies of biological molecules. In addition to providing biological insight, these systems could also prove useful as inspiration for biomimetic materials or devices. A paradigm that has proved to be particularly fruitful consists of integral or peripheral membrane proteins or both, attached to substrates such as lipid multilayer films (formed by the Langmuir–Blodgett technique) and self-assembled monolayers (SAMs) by electrostatic interactions or covalent bonds. Most of the research to date has sought to characterize the structures and physicochemical properties of systems consisting of the peripheral membrane electron transfer protein, cytochrome *c*, attached to thin organic films (Pachence and Blasie, 1987, 1991; Pachence et al., 1989, 1990; Amador et al., 1993; Xu et al., 1993; Chupa et al., 1994; Wang et al., 1994, Delamarche et al., 1995), although analagous studies of the integral membrane proteins such as the photosynthetic reaction center from *R. sphaeroides* (Amador et al., 1993; Chupa et al., 1994) and the Ca^{2+}-ATPase from sarcoplasmic reticulum (Prokop et al., 1996), as well as a reaction center-cytochrome *c* complex (Amador et al., 1993), have also been reported. To set the stage for this paper, which reports molecular dynamics (MD) simulations of cytochrome *c* attached to SAM surfaces, we will now briefly summarize some of the conclusions from the experimental studies of cytochrome *c* attached to thin organic films.

Cytochrome *c* forms two-dimensional, densely packed monolayers when it is electrostatically bound to the negatively charged surfaces of multilayer arachidic acid (AA) Langmuir–Blodgett (LB) (Pachence and Blasie, 1987) or thiolundecanoic acid SAM films (Wang et al., 1994), covalently bound to surface layers of dimyristoylphosphatidylserine (PS) and thioethylstearate (TES) on AA LB films (Pachence et al., 1990) and covalently bound to a hydrolyzed undecylthioacetate SAM surface (Amador et al., 1993; Chupa et al., 1994). The electron-density profiles normal to the surfaces have been determined at up to 7-Å resolution by x-ray diffraction on the AA, AA/dimyristoylphosphatidylserine, and AA/TES LB films (Pachence and Blasie, 1991) and by x-ray interferometry–holography on the thioacetate SAM chemisorbed upon a Ge/Si multilayer substrate (Chupa et al., 1994). The profile structures were consistent with alignment of the major axis of the ellipsoidal protein parallel to the surface (Chupa et al., 1994), and resonance x-ray diffraction revealed that the heme Fe atom is located near the center of the cytochrome *c* profile upon an AA multilayer (Pachence et al., 1989). Moreover, optical linear dichroism measurements have been interpreted in terms of a protein orientation in which the heme is aligned, on average, parallel to the surface but with a large angular distribution or orientational disorder in both electrostatically and covalently bound cytochrome *c* (Pachence et al., 1990). Thus, the unidirectional or "vectorial" orientation (i.e., alignment of a well-defined axis in the molecules) of the protein with respect to the surface has been demonstrated in these systems (Pachence et al., 1990; Chupa et al., 1994). In the case of the AA/TES LB film the electron-density profile suggests that the surface TES layer

Received for publication 7 June 1996 and in final form 11 September 1996.
Address reprint requests to Dr. Michael L. Klein, Department of Chemistry, University of Pennsylvania, Philadelphia, PA 19104-6323. Tel: 215-898-8571; Fax: 215--898-8296; E-mail: klein@lrsm.upenn.edu.

0006-3495/96/12/2933/09 $2.00

is well ordered and that there is a clear separation between the surface and the protein electron densities (Pachence and Blasie, 1991). In contrast, the endgroups in the AA LB film (Pachence and Blasie, 1991) and the thioalkylsiloxane SAM (Chupa et al., 1994) are disordered. There is considerable overlap of the AA surface layer and cytochrome *c* electron densities, suggesting that the protein penetrates the disordered carboxyl headgroup surface to the level of the hydrocarbon chains (Pachence and Blasie, 1987, 1991).

We have performed MD simulations of cytochrome *c* covalently tethered to two SAMs to add some atomic-scale details to the established, experimentally derived picture of these reconstituted membrane systems. There are several issues that we wish to address. Because the chemical identity—and hence the polarity—of the functional groups on the surface of the activated thiol surfaces used in the experimental structural studies to which we will compare our results is unknown (it could be thiol, disulfide, or both (Wasserman et al., 1989)), we have simulated the protein on both hydrophobic and hydrophilic SAM surfaces. Contact angle measurements suggest that the H_2O wetting characteristics, indicative of hydrophobicity-hydrophilicity, are similar on a thioacetate SAM surface before and after hydrolysis (Bain et al., 1989). This suggests that the hydrolyzed surface contains cross-linked disulfide groups because it is less polar than one would expect a thiol surface to be. Therefore, we carried out the simulations with methyl- and thiol-terminated SAMs as limiting cases to investigate to what extent the polarity of surfaces affects protein structure (i.e., compared with the crystal structure and a simulation of the protein alone). Moreover, we speculate, based on comparison of simulation and the experimental results, which of the two surfaces better represents the "real" surfaces. Furthermore, we are interested in how, if at all, the protein affects the structures of the SAMs, and vice versa, and whether the effects, if they exist, are different on the two SAMs. Another issue that we will address that is relevant for the interpretation of experimental data is whether the protein rearranges and penetrates into an organic film with a polar surface, as suggested previously (Pachence and Blasie, 1991; Prokop et al., 1996), at least on the time scale of the simulations (≈1 ns).

MATERIALS AND METHODS

Two systems consisting of one yeast cytochrome *c* molecule covalently tethered to SAMs that comprised 96 $S(CH_2)_{11}X$ molecules were constructed, where, for the hydrophobic surface, $X = CH_3$ and, for the hydrophilic surface, $X = SH$. Considering that the films used in the experiments to which we will compare our results were synthesized with esters in their terminal groups, and assuming that the in-plane chain packing is dictated by the ester moeities, we built our initial SAM configurations based on a monolayer from the known crystal structure of methyl stearate (Aleby and von Sydow, 1960). In this configuration the chains pack in an orthorhombic lattice in the *ab* plane, with $a = 5.61$ Å, $b = 7.33$ Å, and two molecules per unit cell, so that the surface area per chain is 21.56 Å^2. Our SAMs were constructed with 96 chains, truncated to the first 12 methylene units from the stearoyl chain, in a $6b$ (in the x direction) × $8a$ (in the y direction) lattice. A sulfur atom was added to one end of each chain for attachment to the "substrate." In the case of the hydrophobic SAM the terminal methyl group of a chain near the geometric center of the surface was changed to SH to create a site for tethering the the yeast (*S. cerevisiae*) cytochrome *c* by means of a disulfide bond to the surface cysteine residue 102. For the hydrophilic SAM, all the terminal methyl groups were replaced by SH groups. The initial protein configuration was taken from the Protein Data Bank (file 1YCC; Louie and Brayer, 1990), four internal water molecules were retained, and six chloride ions were placed near surface lysine residues for electroneutrality. The protein, water, and ion positions were energy minimized before attachment to the SAMs. During pre-equilibration of the SAMs before the protein was attached, the chain tilt angles with respect to the surface normal decreased from 26° to ~20°, and the tilt directions changed from next-nearest neighbor (along a) to nearest neighbor (along the unit cell diagonal). Molecular graphics images of the initial SAM and protein configurations are shown in Fig. 1.

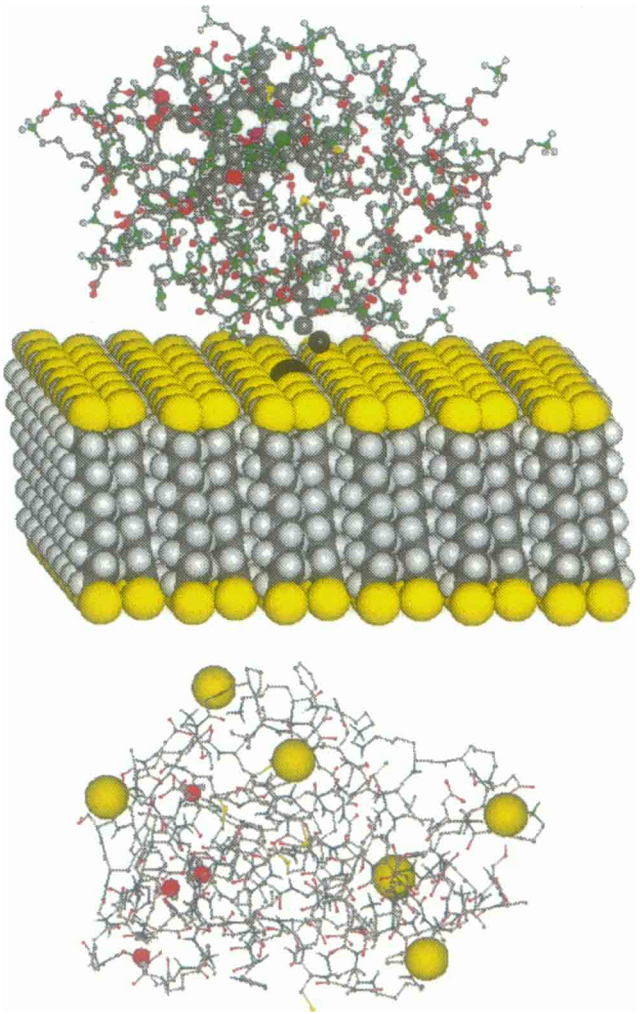

FIGURE 1 (*Top*) Ball-and-stick representation of the x-ray crystal structure of yeast cytochrome *c* above a van der Waals sphere representation of the initial configuration of the thiol-terminated SAM, constructed based on the methyl stearate crystal structure. The protein heme and the surface cysteine residue 102 are shown with enlarged radii. The sulfur atoms used to tether the protein to the SAM by means of a disulfide linkage are colored black. Otherwise, the atom coloring scheme is C, gray; H, white; O, red; N, green; S, yellow; and Fe, magenta. (*Bottom*) Ball-and-stick representation of the initial protein configuration after energy minimization with the six neutralizing chloride ions and four internal water molecules shown with enlarged radii (here the ions are also colored yellow).

To model the hydrocarbon parts of the molecules that compose the SAMS we used an all-atom potential that well reproduces the structures of solid and liquid alkanes (D. J. Tobias, K. Tu, and M. L. Klein, unpublished) and is very similar to a potential used in a recent simulation study of pentadecanethiol SAMs (Mar and Klein, 1994). A harmonic potential with a force constant of 235.5 (kcal/mol)/Å^2 (98,530 (kJ/mol)/nm^2), roughly that of a C—C bond, was used to keep the adsorbed S atoms near their initial lattice sites. Unlike in previous studies of modeling SAMs of alkanethiols (Hautman et al., 1991; Mar and Klein, 1994), no surface van der Waals and corrugation potentials were included in our calculations. The thiol groups were modeled with the explicit hydrogen representation of Jorgensen (1986), and the protein with the "polar H" CHARMM PARAM19 potential (Reiher, 1985). The TIP3P model was used for the water molecules (Jorgensen et al., 1983), and the potential of Buckner and Jorgensen (1989) for the chloride ions. Periodic boundary conditions were employed in the simulations to infinitely replicate the SAM–protein systems in two dimensions, and an Ewald summation method for planar systems (Hautman and Klein, 1992) was used to calculate the electrostatic interactions (using α = 0.15, G_{max} = 39, ν = 0). The van der Waals interactions were calculated by use of the minimum-image convention with spherical truncation at 10 Å (Allen and Tildesley, 1989). All the nonbonded interactions were included without truncation in a control simulation of the protein in vacuum.

After constructing the systems as described above, we performed MD simulations of cytochrome *c* at constant temperature (T = 27°C) for 1160 ps on the methyl-terminated SAM, 1070 ps on the thiol-terminated SAM, and 600 ps in vacuum. The temperature was controlled by the Nosé–Hoover chain method (Martyna et al., 1992), with separate thermostats on the SAM and the protein atoms. We integrated the equations of motion with an iterative Verlet-like algorithm (Ciccotti and Ryckaert, 1986), using a time step of 1.5 fs, and the SHAKE algorithm (Ryckaert et al., 1977) was used to constrain the lengths of bonds involving hydrogen atoms. The fictitious masses of the thermostat variables were chosen according to the prescription given by Martyna et al. (1992), with time scales of 0.5 ps. The Nosé–Hoover thermostat chain length was five. The calculations were performed with the CHARMM program (Brooks et al., 1983), version 23, as modified by us to implement the constant temperature dynamics and planar Ewald summation. The convergence of the SAM–protein trajectories was slow because of the long-time-scale rearrangement of the protein on the surfaces. Judging from the time evolution of the deviation of the protein from the x-ray crystal structure, we decided to use only the last 300 ps from each run for analysis. The calculations were carried out on an IBM SP1 computer at the Cornell Supercomputing Center and on Silicon Graphics R4000 workstations at the University of Pennsylvania.

Before moving on to the results, keeping in mind that we are interested primarily in qualitative observations in this initial investigation, we want to point out some obvious differences between real and simulated systems. Perhaps the most significant difference is that the samples used in the experiments were maintained at 98% humidity, whereas with the exception of the four internal water molecules the simulated systems were left completely dry for computational expediency. Another significant difference is that the protein molecules are densely packed in the real samples but the simulations were set up at a packing fraction of ~50% and therefore do not contain the effects of protein–protein contacts. Finally, the details of the in-plane structure of the films actually used in the experiments have not been determined; hence we made the assumptions stated above to set up our model SAMs.

RESULTS AND DISCUSSION

In Table 1 we show averages taken over the last 300 ps of the simulations for the root-mean-square deviation (rmsd) of the α carbon positions from the crystal structure, radius of gyration (R_g), eccentricity, and orientation of the heme plane with respect to the surfaces, along with available experimental results for comparison. During the ≈1000-ps simulations on the SAMs, the rmsd, R_g, and the eccentricity required ~650 ps to converge relative to their initial (crystal structure) values, whereas the heme angle converged in ~600 ps and ~200 ps on the methyl- and thiol-terminated SAMs, respectively. The rmsd of ~2 Å in the control calculation is typical for a vacuum simulation of a globular protein. The increased rmsds of the protein on the SAMs indicate significant structural changes resulting from interactions with the surfaces (see below). The control protein is more compact (has a smaller radius of gyration) than the crystal structure. This "electrostriction" is typical for a simulation of a globular protein in vacuum in which, in the absence of solvent, protein–protein contacts, or both, the polar sidechains that normally protrude from the exterior of the protein have no choice but to reach back and interact

TABLE 1 Results for protein structural quantities

Quantity	CH_3 SAM*	SH SAM*	Control*	Expt.
C^α rmsd (Å)#	3.2	2.9	1.9	
R_g (Å)	12.8	13.0	12.6	13.0§
Eccentricity	0.20	0.24	0.16	0.18§
Heme orientation (°)	36	66		≈0¶

*Averages over last 300 ps MD.
#Root-mean-squared deviation versus the x-ray crystal structure.
§Calculated from the x-ray crystal structure (Louie and Brayer, 1990).
¶Optical linear dichroism (Pachence et al., 1990).

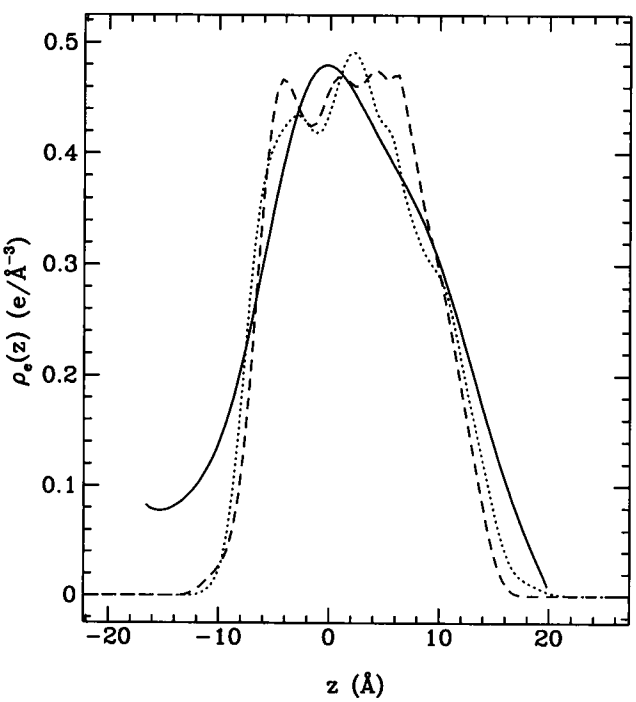

FIGURE 2 Electron-density profile derived from x-ray diffraction data by Chupa et al. (1994) on cytochrome *c* covalently tethered to a hydrolyzed thioacetate SAM (*solid curve*) and profiles for the protein only from MD simulations of cytochrome *c* on methyl- (*dotted curve*) and thiol-terminated (*dashed curve*) SAMs.

with each other or the backbone. The radius of gyration on the hydrophilic surface is the same as in the crystal and is only slightly smaller on the hydrophobic surface. However, the eccentricity, defined as $1 - I_{max}/I_{avg}$, where I_{max} is the maximum and I_{avg} is the average of the principal moments of inertia, signals significant protein shape changes on the surfaces. The control protein becomes slightly more spherical than the crystal structure (eccentricity = 0 for a sphere) but more ellipsoidal than the control on the surfaces, more so on the thiol-terminated than on the methyl-terminated SAM. The heme plane, which was at an angle of 50° with respect to the surfaces in the initial configurations, ended up more nearly parallel (36°) to the hydrophobic surface and more nearly perpendicular (66°) to the hydrophilic surface. Pachence et al. (1990) experimentally studied the heme orientation in cytochrome *c* covalently bound to the surface of an AA/TES film by measuring the dichroic ratio for the heme optical absorption. The data were initially interpreted as indicating that the heme plane is more parallel than perpendicular to the surfaces. In fact, according to the theory of Blasie et al. (1978), an unphysical spread in the heme orientational distribution would be required for the average heme orientation to be strictly parallel to the TES monolayer plane. Using the value ≈0.80, measured for the dichroic ratio at an angle of incidence of 45°, we read a heme angle of ≈42° for reasonable values of the mosaic spread (10°–30°) from Fig. 5 of Blasie et al. (1978). A very similar result was obtained recently by use of good signal-to-noise ratio data on cytochrome *c* covalently tethered to a hydrolyzed thioacetate SAM (A. M. Edwards and J. K. Blasie, unpublished results). Thus, the values obtained from the experiments on cytochrome *c* covalently bound to activated thiol surfaces are similar to the 36° from the simulation on the methyl-terminated SAM but significantly differ

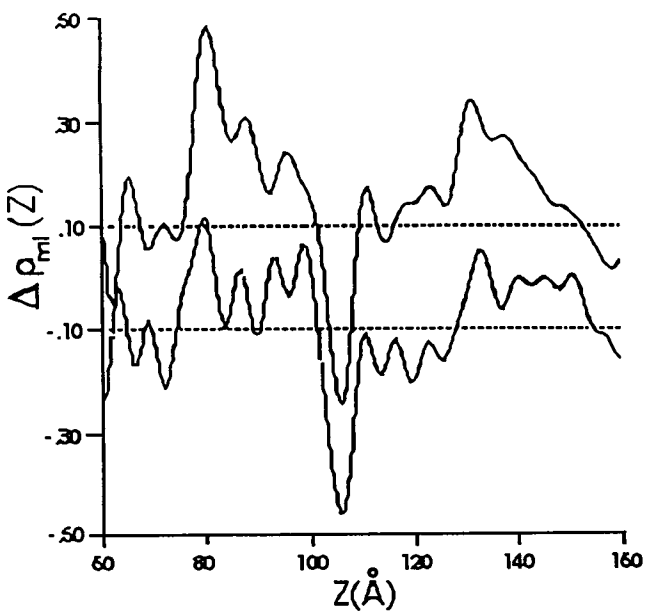

FIGURE 3 Multilayer relative electron-density profiles, $\Delta\rho_{ml}(z)$, for the surface lipid monolayer and the next underlying monolayer from x-ray diffraction (Pachence and Blasie, 1991): AA–TES (*top*); AA–TES–cytochrome *c* (*bottom*). The AA and TES layers are separated by a terminal methyl trough at $z \approx 105$ Å. The underlying AA layer is at $z = 80$ Å $\leq$ 105 Å, the surface TES layer at 105 Å $z \leq 135$ Å, and the cytochrome *c*, covalently tethered through a disulfide linkage with cysteine-102, at 135 Å $\leq$ 160 Å (*bottom*). The TES carboxyl group lies at $z \approx 130$ Å and the TES thiol endgroup at $z \approx 135$ Å in these profiles.

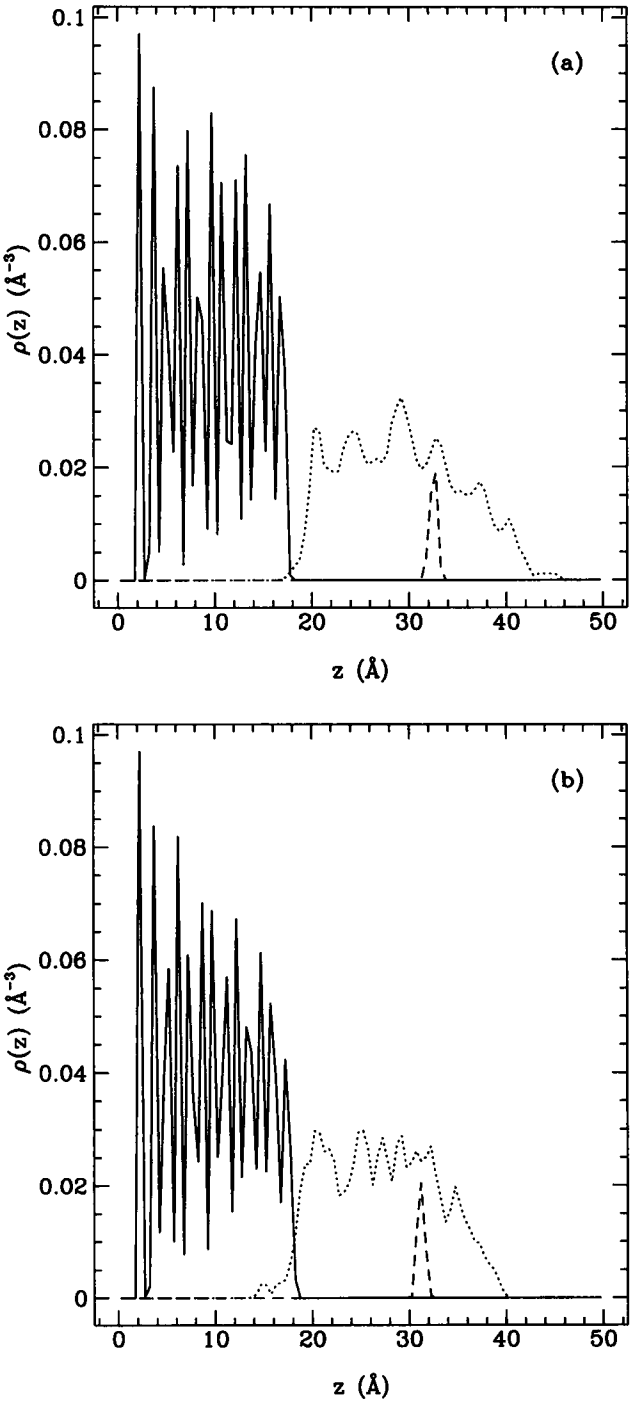

FIGURE 4 Atomic-number density profiles for the SAM carbon and sulfur (*solid curves*), protein (*dotted curves*), and heme iron atoms (*dashed curves*; after multiplication by 40): (*a*) methyl-terminated SAM, (*b*) thiol-terminated SAM.

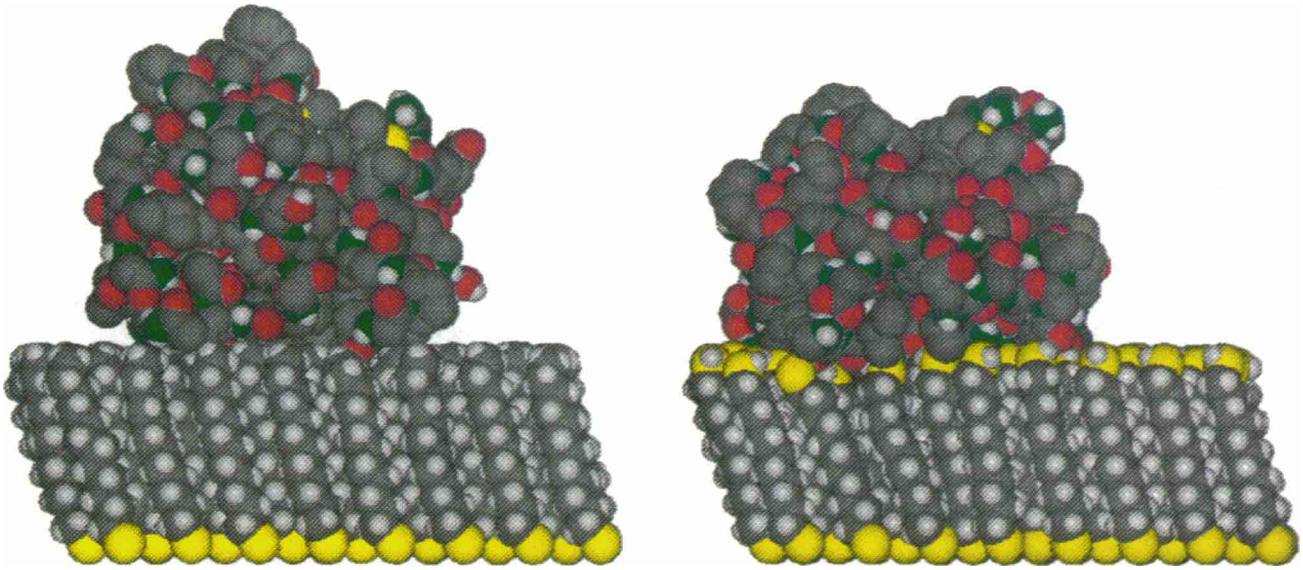

FIGURE 5 Snapshots from MD simulations of cytochrome *c* on methyl-terminated (*left*) and thiol-terminated (*right*) SAMs. The coloring scheme is as in Fig. 1.

ent from the 66° from the simulation on the thiol-terminated SAM. This suggests that the "real" surfaces to which the protein is covalently bound are nonpolar; i.e., the SH endgroups are oxidized to form an SS cross-linked surface. The dichroic ratio, and hence the heme orientation, measured for horse heart cytochrome *c* electrostatically bound to the polar surface of an AA LB film is very similar to that for the protein covalently bound to the presumably nonpolar activated thiol surfaces (Pachence et al., 1990) but is not directly comparable with our result for the protein covalently bound to the polar thiol-terminated SAM.

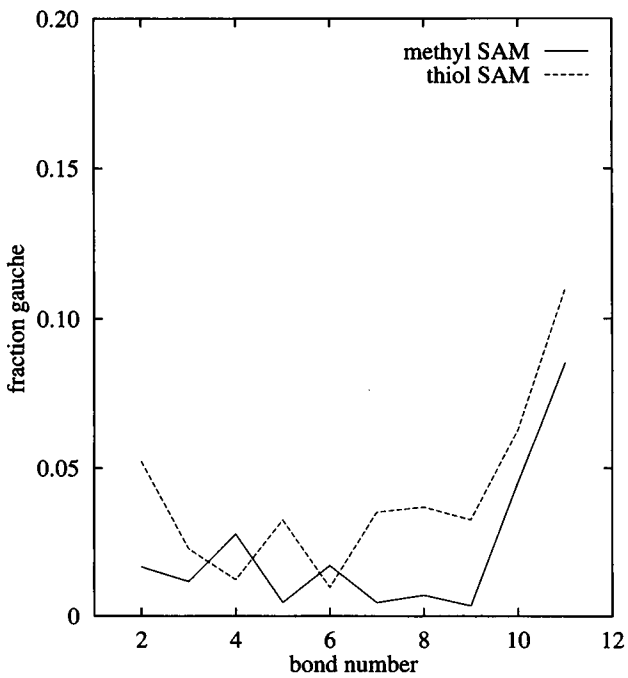

FIGURE 6 Fraction *gauche* conformations versus bond number in the methyl- (*solid curve*) and thiol-terminated (*dashed curve*) SAMs.

In Fig. 2 we compare the electron-density profiles from the simulations with the profile derived from x-ray interferometry–holography by Chupa et al. (1994). These profiles can be compared with the relative electron-density profiles shown in Fig. 3 derived by Pachence and Blasie (1991) from x-ray diffraction on surface layers of TES and TES/cytochrome *c* on AA LB films. We computed the profiles from the simulation data (for the protein only) by placing a Gaussian distribution of electrons on each atomic center with a variance equal to the van der Waals radius, calcuating the density for each configuration, and averaging over configurations. The width of the protein is 20 Å in all the profiles and is consistent with the long axis of the approximately ellipsoidal protein oriented parallel to the SAM surface (Chupa et al., 1994). The profile of Chupa et al. (1994) is smoother and broader than the others because the SAM to which it is tethered is less ordered than those modeled in the simulations. Nevertheless, the shape of this experimental profile shows better agreement with the profile from the simulation on the hydrophobic surface. However, from the electron-density profiles of the protein alone it is not possible to resolve a precise correspondence between the experimental and simulated systems.

In Fig. 4 we show the protein and SAM atomic-number density distributions from the simulations. The sharp peaks in the SAM distributions show that both SAMs remained well ordered in the simulations. The peaks near the ends of the chains are a little sharper in the methyl-terminated SAM, indicating slightly more order. There is a clear separation between the methyl-terminated SAM and the protein densities, but the protein density overlaps the thiol-terminated

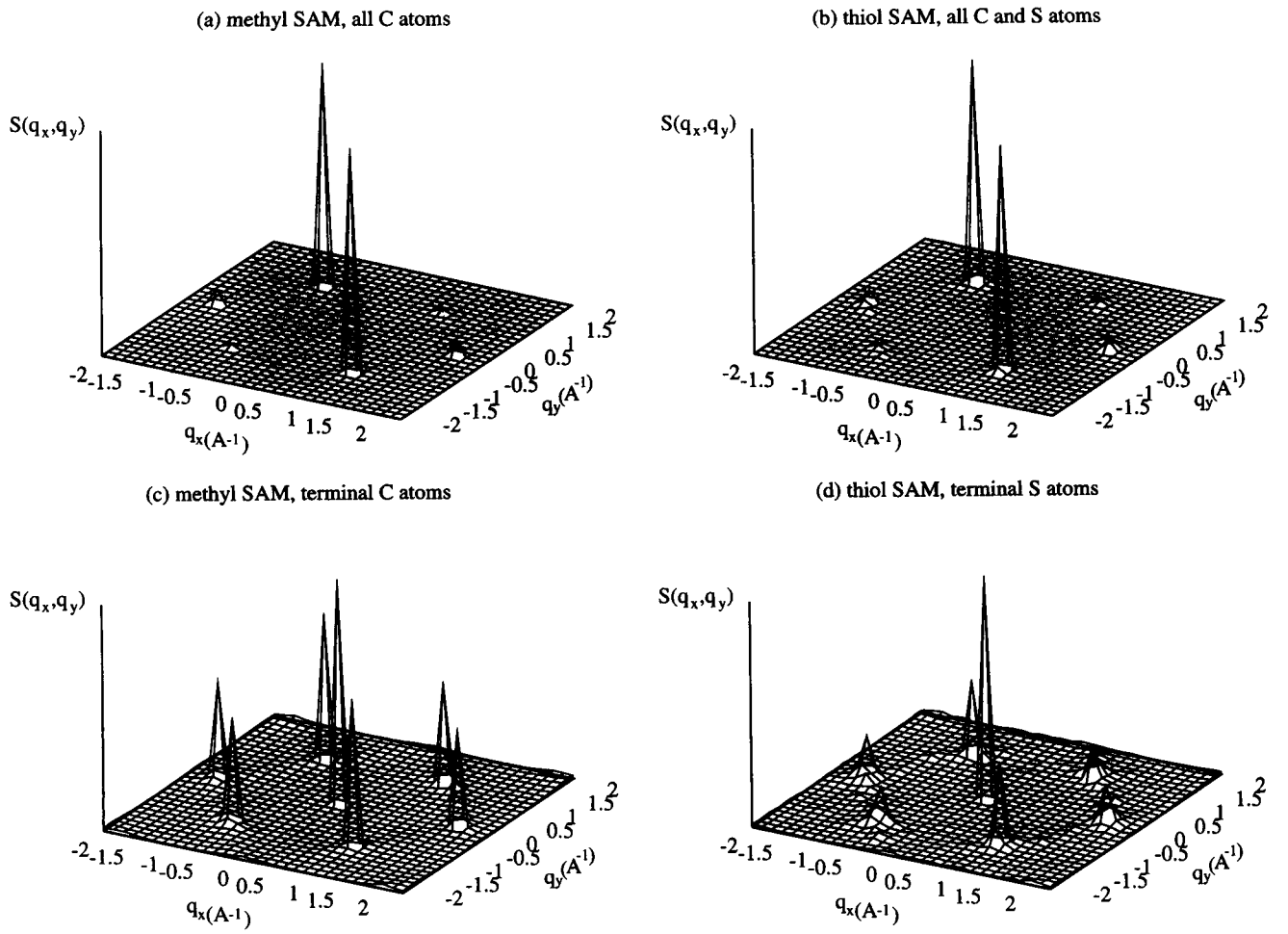

FIGURE 7 In-plane structure factors: (*a*) all atoms, methyl-terminated SAM; (*b*) all atoms, thiol-terminated SAM; (*c*) terminal methyl C atoms; (*d*) terminal thiol S atoms.

SAM density by ≈5 Å. Thus, the protein is completely excluded from the hydrophobic surface but partially "dissolves" into the hydrophilic surface. The former situation is analogous to that observed in the experimental electron density profile for yeast cytochrome *c* covalently bound to TES (see Fig. 3), and the latter to that for horse heart cytochrome *c* electrostatically bound to AA (cf. Fig. 4 *C* in Pachence and Blasie, 1990). The heme iron atom density is centered ~15 Å beyond the terminal methyl of the hydrophobic SAM and ~13 Å beyond the terminal sulfur atom of the hydrophilic SAM, with a narrow distribution (full width at half-maximum of ≈1 Å) in both cases. Both of these values lie within the 15 ± 2 Å region measured by a resonance x-ray diffraction experiment on cytochrome *c* electrostatically bound to AA (Pachence et al., 1989).

Several of the features noted thus far are evident in the snapshots from the simulations shown in Fig. 5. It is obvious from the figure that the shape of the protein is significantly different on the two SAMs. Roughly in analogy to the difference in the microscopic wetting behavior of water on hydrophobic and hydrophilic SAM surfaces (Hautman and Klein, 1991), the polar sidechains of the protein "wet" the polar SAM surface, whereas the protein looks more like a droplet on the nonpolar surface. It appears from the figure that the protein has little effect on the structure of the methyl SAM, whereas the structure of the thiol SAM is perturbed beneath the protein.

In spite of this local perturbation, which we examine in more detail below, overall measures of the chain structure suggest that the structures of the two SAMs are similar. In particular, the chains in both SAMs maintained a collective nearest-neighbor tilt direction, with an average tilt angle of 20° in the methyl-terminated and 17° in the thiol-terminated SAM. Fig. 6 shows that there are very few *gauche* conformations in the middles of the chains of both SAMs and that the ends of the chains have only slightly more *gauche* defects in the thiol-terminated SAM. The average tilt angles and *gauche* fractions in the two $S(CH_2)_{11}X$ SAMs at 27°C are in the range of those observed in a simulation of an $S(CH_2)_{14}CH_3$ SAM at 60°–70°C (Mar and Klein, 1994). The similarity of the gross structures of the methyl- and thiol-terminated SAMs is illustrated in Fig. 7*A* and *B*, where

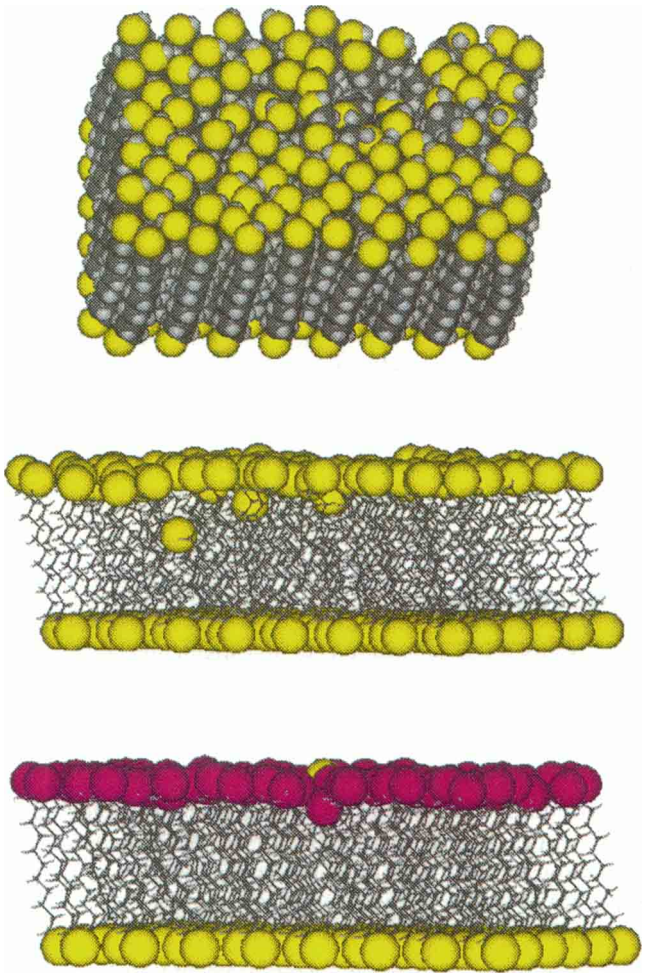

FIGURE 8 (*Top*) Top and (*middle*) side views of the thiol-terminated SAM and (*bottom*) side view of the methyl-terminated SAM. The coloring scheme is as in Fig.1, except that the terminal methyl groups of the hydrophobic SAM are colored magenta.

we have plotted the in-plane structure factors, $S(\mathbf{q})$, calculated for the chain heavy atoms:

$$S(\mathbf{q}) = \langle \exp(i\mathbf{q} \cdot \mathbf{r}_i) \exp(-i\mathbf{q} \cdot \mathbf{r}_i) \rangle,$$

where $\mathbf{q} = (q_x, q_y)$, $q_x = 2\pi h/L_x$, $q_y = 2\pi k/L_y$, L_x and L_y are the lengths of the simulation cell in the x and the y directions, respectively, h and k are integers, and the angle brackets denote an average over time and the N atoms. The presence of essentially only two peaks in these structure factors is a manifestation of the chain tilt. The structure factors calculated for the terminal methyl C and thiol S atoms plotted in Fig. 7 *C* and *D* show that, in spite of the similarity of the overall packing of the chains in the two SAMs, the degree of ordering in the terminal groups is significantly greater at the hydrophobic surface. The difference in the ordering of the endgroups on the two surfaces is analgous to that between the AA/TES and the pure-AA LB films studied experimentally by Pachence and Blasie (1990).

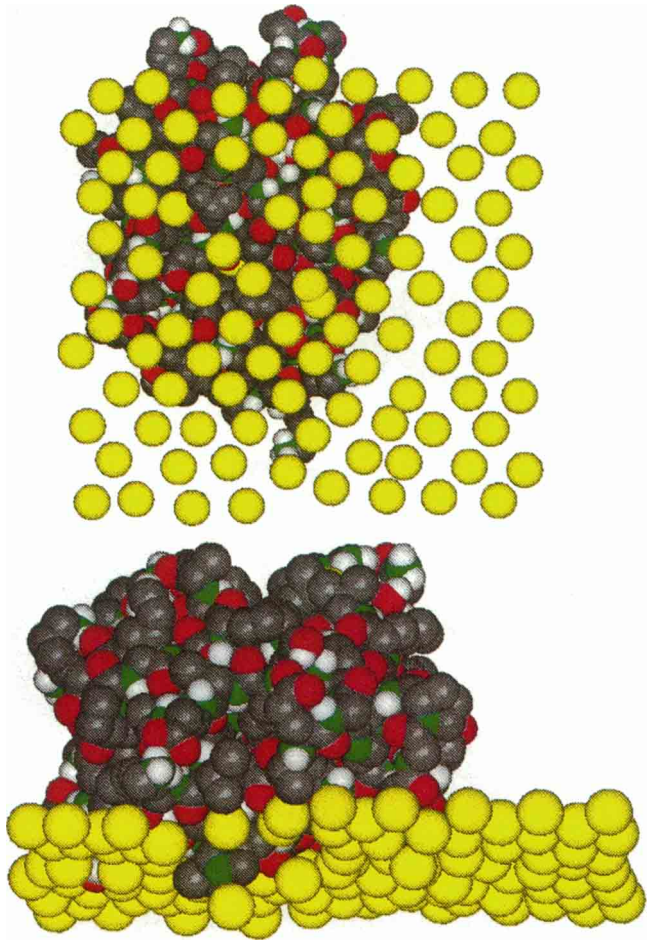

FIGURE 9 View of the cytochrome *c* (*top*) from below and (*bottom*) from the side of the surface layer of S atoms in the thiol-terminated SAM. The coloring scheme is as in Fig. 1.

On closer inspection it is evident that penetration by the protein is responsible for the greater disorder at the surface of the thiol-terminated SAM (Figs. 8 and 9). From Fig. 8 one can see that the protein creates several holes in the hydrophilic surface by depressing thiol groups and forcing *gauche* defects in the chains. One of the holes is large enough to expose a sizable patch of methylene groups. In contrast, the hydrophobic surface of the methyl-terminated SAM remains flat, except for the depression of one methyl group next to the protein attachment site. The protein sidechains responsible for creating the holes are evident in Fig. 9. The deepest holes are occupied by a nonpolar leucine sidechain and the nonpolar part of a histidine sidechain. In the case of the histidine, the sidechain $N^{\epsilon 2}$ atom maintains a hydrogen bond with a thiol group that has been pushed deeply into the interior of the SAM. With the exception of the hydroxyl group of a threonine sidechain that penetrates just beneath the level of the sulfur atoms, the strongly polar groups in the protein appear to interact preferentially with the hydrophilic surface from above.

On the time scale of the simulations ($\approx$1 ns), the protein effects on the structures of the SAMs, where they exist, are

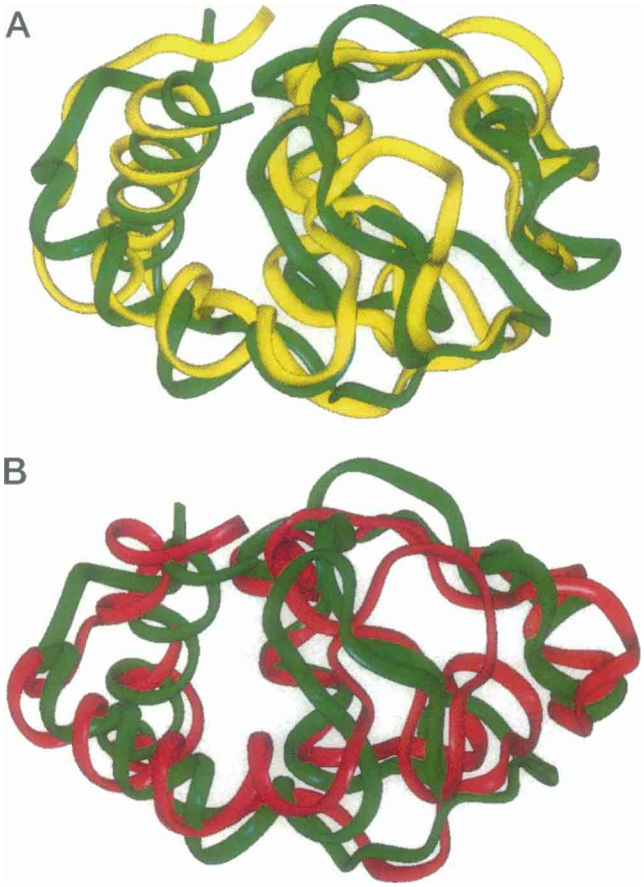

FIGURE 10 Ribbon representations of snapshots of the cytochrome *c* backbone: (*a*) from the simulation on the methyl-terminated SAM (*yellow*) and the crystal structure (*green*); (*b*) from the simulation on the thiol-terminated SAM (*red*) and the crystal structure (*green*). The pairs of structures were superimposed by least-squares fitting the C^{α} positions.

quite local in character. Conversely, it appears that the effects of interactions with the surfaces on the structure of the protein are also minor and do not involve any large-scale conformational changes (e.g., unfolding). This is illustrated by the ribbon diagrams in Fig. 10, from which it is clear that the overall fold of cytochrome *c* is preserved on both of the surfaces. The essentially all-α helical secondary structure remains intact, although the relative orientation (packing) of the three longest helices and the placement of the loops have been modified slightly relative to the crystal structure. The hydrogen bonding in the small (four H-bond) β sheet has not been disrupted by either surface, although the hairpin loop containing the sheet has been displaced. Overall, the surface-induced changes in protein structure appear to be slightly greater on the hydrophobic surface, as expected from the data in Table 1.

Before concluding, we briefly compare the protein structures from our simulations with results from a simulation by Wong et al. (1993) of tuna cytochrome *c* in water, keeping in mind that a quantitative comparison is unwarranted given the differences in the protein sequence, potential parameters, and calculation of electrostatic interactions. The primary difference is that the protein expanded slightly relative to the crystal structure in the solution simulation of Wong et al., judging from the radius of gyration and solvent-accessible surface area (SASA), whereas it contracted in our simulations: Wong et al. observed a slight increase in R_{gyr} and an 11% increase in SASA relative to the crystal structure, whereas we found decreases in SASA of 10% on the hydrophobic surface, 5% on the hydrophilic surface, and 10% in the control. Moreover, the rmsd in the solution simulation was less than in our simulations. Finally, Wong et al. noted appreciable fluctuations in the SASA, $\approx$4% over 100 ps, whereas the fluctuations were less than 1% over 100 ps in all our simulations; i.e., the surface of the protein is more fluid in solution than in vacuum, where the polar sidechains are rigidly held in place by unscreened electrostatic interactions with each other.

CONCLUSIONS

We have used MD simulations to investigate the behavior of a peripheral membrane protein, cytochrome *c*, covalently tethered to hydrophobic (methyl-terminated) and hydrophilic (thiol-terminated) self-assembled monolayers. The simulations predict that the protein will undergo minor, but significant, overall structural changes when it is tethered to either surface, and the structures differ qualitatively on the two surfaces: The protein is less spherical on the hydrophilic SAM where the polar surface residues reach out to interact with the SAM surface. This is analogous to the difference in the microscopic wetting behavior of water on hydrophobic and hydrophilic surfaces (Hautman and Klein, 1991). The protein is completely excluded from the hydrophobic SAM but partially dissolves in the hydrophilic SAM. Consequently, the surface of the thiol-terminated SAM is considerably less ordered than that of the methyl-terminated SAM, although a comparable, high degree of order is maintained in the bulk of both SAMs: The chains exhibit collective tilts in the nearest-neighbor direction at angles of 20° and 17° with respect to the surface normal in the hydrophobic and the hydrophilic SAMs, respectively. On the hydrophobic SAM the protein is oriented so that the heme plane is more nearly parallel to the surface, whereas on the hydrophilic surface it is more perpendicular. The secondary structure of the protein, dominated by α helices, is not significantly affected, but the structure of the loops as well as that of helix packing is slightly modified by the surfaces.

Considering the structural features best characterized in the experimental investigations of cytochrome *c* on thin organic films, namely, the extent of protein–surface overlap, heme orientation, and the order of the chains that constitute the film, the closest correspondence between the simulated and the real systems is that between the simulated methyl-terminated SAM and the AA/TES LB film of Pachence and Blasie (1990). The qualitative similarity of these systems suggests that the real surface to which the protein is covalently tethered in the experiments is nonpo

lar, i.e., is composed of cross-linked disulfide as opposed to free-thiol groups.

As we pointed out in the Introduction, there are several limitations within this initial modeling attempt that preclude a quantitative comparison with the experimentally studied systems. Improvements in future attempts should include hydration, higher protein packing fraction (i.e., to incorporate protein–protein contact effects), and a more direct representation of the particular film(s) employed in the experiments. Nonetheless, this preliminary investigation provides some useful qualitative atomic-scale insight into the nature and consequences of globular protein interactions with hydrophobic and hydrophilic surfaces.

We are grateful to Mounir Tarek for assistance in preparing some of the figures. This research was supported by the National Institutes of Health through grants R01 GM40712 (M.L.K.), R01 GM33525 (J.K.B.), and F32 GM14463 (D.J.T.). Some of the calculations were performed on the IBM SP1 computer at the Cornell Supercomputing Center under Metacenter Allocation MCA93S020.

REFERENCES

Aleby, S., and E. von Sydow. 1960. The crystal structure of methyl stearate. *Acta Crystallogr.* 13:487–492.

Allen, M. P., and D. J. Tildesley. 1989. Computer Simulation of Liquids. Oxford University Press, New York.

Amador, S. M., J. M. Pachence, R. Fischetti, J. P. McCauley, Jr., A. B. Smith III, and J. K. Blasie. 1993. Use of self-assembled monolayers to covalently tether protein monolayers to the surface of solid substrates. *Langmuir.* 9:812–817.

Bain, C. D., E. B. Troughten, Y.-T. Tao, J. Evall, G. M. Whitesides, and R. G. Nuzzo. 1989. Formation of monolayer films by the spontaneous assembly of organic thiols from solution onto gold. *J. Am. Chem. Soc.* 111:321–335.

Blasie, J. K., M. Erecinska, M., S. Samuels, and J. S. Leigh. 1978. The structure of a cytochrome *c* oxidase-lipid model membrane. *Biochim. Biophys. Acta.* 501:33–52.

Brooks, B. R., R. E. Bruccoleri, B. D. Olafson, D. J. States, S. Swaminathan, and M. Karplus. 1983. CHARMM: a program for macromolecular energy, minimization, and dynamics calculations. *J. Comp. Chem.* 4:187–217.

Buckner, J. K., and W. L. Jorgensen. 1989. Energetics and hydration of the constituent ion pairs of tetramethylammonium chloride. *J. Phys. Chem.* 111:2507–2516.

Chupa, J. A., J. P. McCauley, Jr., R. M. Strongin, A. B. Smith III, J. K. Blasie, L. J. Peticolas, and J. C. Bean. 1994. Vectorially oriented membrane protein monolayers: profile structures via x-ray interferometry/holography. *Biophys. J.* 67:336–348.

Ciccotti, G., and J.-P. Ryckaert. 1986. Molecular dynamics simulation of rigid molecules. *Comp. Phys. Rep.* 4:347–392.

Delamarche, E., H. Biebuyck, B. Michel, G. Sundarababu, H. Sigrist, H. Wolf, and H. Ringsdorf. 1995. STM analysis of cytochrome *c* immobilized on self-assembled monolayers on gold. *In* Procedures in Scanning Probe Microscopies. R. Colton et al., editors. John Wiley & Son, Chichester, UK.

Hautman, J., J. P. Bareman, W. Mar, and M. L. Klein. 1991. Molecular dynamics investigation of self-assembled monolayers. *J. Chem. Soc. Faraday Trans.* 87:2031–2037.

Hautman, J., and M. L. Klein. 1991. Microscopic wetting phenomena. *Phys. Rev. Lett.* 13:1763–1766.

Hautman, J., and M. L. Klein. 1992. An Ewald summation method for planar surfaces and interfaces. *Mol. Phys.* 75:379–395.

Jorgensen, W. L. 1986. Intermolecular potential functions and Monte Carlo simulations for liquid sulfur compounds. *J. Phys. Chem.* 90:6379–6388.

Jorgensen, W. L., J. Chandrasekhar, J. D. Madura, R. W. Impey, and M. L. Klein. 1983. Comparison of simple potential functions for simulating liquid water. *J. Chem. Phys.* 79:926–935.

Louie, G. V., and G. D. Brayer. 1990. High-resolution refinement of yeast iso-1-cytochrome *c* and comparison with other eukaryotic cytochromes *c*. *J. Mol. Biol.* 214:527–555.

Mar, W., and M. L. Klein. 1994. Molecular dynamics study of the self-assembled monolayer composed of $S(CH_2)_{14}CH_3$ molecules using an all-atoms model. *Langmuir.* 10:188–196.

Martyna, G. J., M. L. Klein, and M. Tuckerman. 1992. Nosé–Hoover chains: the canonical ensemble via continuous dynamics. *J. Chem. Phys.* 97:2635–2643.

Pachence, J. M., S. Amador, G. Maniara, J. Vanderkooi, P. L. Dutton, and J. K. Blasie. 1990. Orientation and lateral mobility of cytochrome *c* on the surface of ultrathin lipid multilayer films. *Biophys. J.* 58:379–389.

Pachence, J. M., and J. K. Blasie. 1987. The location of cytochrome *c* on the surface of ultrathin lipid multilayer films using x-ray diffraction. *Biophys. J.* 52:735–747.

Pachence, J. M., and J. K. Blasie. 1991. Structural investigation of the covalent and electrostatic binding of yeast cytochrome *c* to the surface of various ultrathin lipid multilayers using x-ray diffraction. *Biophys. J.* 59:894–900.

Pachence, J. M., R. F. Fischetti, and J. K. Blasie. 1989. Location of the heme-Fe atoms within the profile structure of a monolayer of cytochrome *c* bound to the surface of an ultrathin lipid multilayer film. *Biophys. J.* 327–337.

Prokop, L. A., R, M. Strongin, A. B. Smith III, and J. K. Blasie. 1996. Vectorially oriented monolayers of detergent-solubilized Ca^{2+}-ATPase from sarcoplasmic reticulum. *Biophys. J.* 70:2131–2143.

Reiher, W. E. 1985. Theoretical Studies of Hydrogen Bonding. Ph.D. dissertation, Harvard University, Cambridge, MA.

Ryckaert, J.-P., G. Ciccotti, and H. J. C. Berendsen. 1977. Numerical integration of the Cartesian equations of motion of a system with constraints: molecular dynamics of *n*-alkanes. *J. Comp. Phys.* 23: 327–341.

Wang, J., C. J. A. Wallace, I. Clark-Lewis, and M. Caffrey. 1994. Structure characterization of membrane bound and surface adsorbed protein. *J. Mol. Biol.* 237:1–4.

Wasserman, S. R., H. Biebuyck, and G. M. Whitesides. 1989. Monolayers of 11-trichlorosilylundecyl thioacetate: a system that promotes adhesion between silicon dioxide and evaporated gold. *J. Mater. Res.* 4:886–892.

Wong, C. F., C. Zheng, J. Shen, J. A. McCammon, and P. G. Wolynes. 1993. Cytochrome *c*: a molecular proving ground for computer simulations. *J. Phys. Chem.* 97:3100–3110.

Xu, S., R. F. Fischetti, J. K. Blasie, L. J. Peticolas, and J. C. Bean. 1993. Profile and in-plane structures of self-assembled monolayers on Ge/Si multilayer substrates by high-resolution x-ray diffraction employing x-ray interferometry/holography. *J. Phys. Chem.* 97:1961–1969.